

Organic & Biomolecular Chemistry

Accepted Manuscript



This is an *Accepted Manuscript*, which has been through the Royal Society of Chemistry peer review process and has been accepted for publication.

Accepted Manuscripts are published online shortly after acceptance, before technical editing, formatting and proof reading. Using this free service, authors can make their results available to the community, in citable form, before we publish the edited article. We will replace this *Accepted Manuscript* with the edited and formatted *Advance Article* as soon as it is available.

You can find more information about *Accepted Manuscripts* in the [Information for Authors](#).

Please note that technical editing may introduce minor changes to the text and/or graphics, which may alter content. The journal's standard [Terms & Conditions](#) and the [Ethical guidelines](#) still apply. In no event shall the Royal Society of Chemistry be held responsible for any errors or omissions in this *Accepted Manuscript* or any consequences arising from the use of any information it contains.

Advances in 1-phenanthryl-tetrahydroisoquinoline series of PAK4 inhibitors: Potent agent restrains tumor cell growth and invasion

Chenzhou Hao,^{‡a} Xiaodong Li,^{‡b} Shuai Song,^a Bingyu Guo,^b Jing Guo,^a Jian Zhang,^b Qiaoling Zhang,^a Wanxu Huang,^a Jian Wang,^a Bin Lin,^a Maosheng Cheng,^{*a} Feng Li^{*b} and Dongmei Zhao^{*a}

^a Key Laboratory of Structure-Based Drug Design & Discovery of Ministry of Education, Shenyang Pharmaceutical University, Shenyang 110016, China. E-mail: mscheng@263.net, dongmeiz-67@163.com; Fax: +86-24-23995043; Tel: +86-24-23986413

^b Department of Cell Biology, Key Laboratory of Cell Biology, Ministry of Public Health, and Key Laboratory of Medical Cell Biology, Ministry of Education, China Medical University, Shenyang 110001, China. E-mail: fli@mail.cmu.edu.cn; Fax: +86-24-23261056; Tel: +86-24-23256666

[‡] These authors contributed equally to this work.

New series of novel 1-phenanthryl-tetrahydroisoquinoline derivatives were designed, synthesized and biologically evaluated for their PAK4 inhibitory activities and anti-proliferative effects against three cancer cell lines A549, MCF-7 and HT-1080. Among them, compound **12a** exhibited the most potent inhibitory activity against PAK4 with IC₅₀ of 0.42 μM. Moreover, this compound inhibited the invasion of A549 tumor cells by regulating PAK4-LIMK1-Cofilin signaling pathway *in vitro*, and exhibited anti-tumor activity *in vivo* in the A549 tumor xenograft model. To further evaluate the binding mode of **12a** with PAK4, biotinylated **12a** derivative has been synthesized and was used for immunoprecipitation assay. Intriguingly, our observations suggest that **12a** interactions with both the N- and C-termini of PAK4.

Introduction

The p21-activated kinases (PAKs) are serine/threonine kinases that have been extensively studied and shown to play significant roles in cancer progression since their discovery in 1994.¹ The majority of cellular processes attributed to PAKs induce reorganization of the actin cytoskeleton downstream of Rho family GTPases, Cdc42 and Rac.² PAKs have been implicated to control many cellular functions, such as cytoskeletal signaling pathway,³ cytoskeletal reorganization,⁴ cell motility,⁵ morphological changes,⁶ and cell-cycle progression.⁷ The PAKs are divided into two groups, group I (PAK1-3) and group II (PAK4-6), based on their domain organizations and regulatory properties. All PAKs share a number of conserved structural characteristics, including an N-terminal GTPase-binding domain (GBD) with an overlapping auto-inhibitory domain (AID),⁸ and a C-terminal serine/threonine kinase domain.⁹ However, the kinase domains of group I and II PAKs only share approximately 50% identity, suggesting that these groups may recognize different substrates and govern unique cellular processes.¹⁰⁻¹² In contrast to the well-characterized group I PAKs, research on group II PAKs is still in its infancy.

PAK4 is widely expressed and most abundant in prostate, testis, and colon.^{5, 13} Based on nearly two decades of research, PAK4 has been shown to participate in progression of cancer. Gene amplification,¹⁴⁻¹⁶ protein overexpression^{17, 18} and mutation¹⁴ of PAK4 were the major characteristics in a variety of tumors. It was reported that PAK4 activation (phosphorylation on Ser474) correlates with poor prognosis in human gastric cancer patients.¹⁹ Increased expression of PAK4 was associated with metastasis, shorter overall survival, advanced stage of human non-small cell lung cancer.²⁰ The mechanism of PAK4 regulated tumor progression has been well studied. PAK4 promoted cancer cell migration by regulating the actin cytoskeleton through not only phosphorylation of the guanine nucleotide exchange factor H1 (GEF-H1) but also LIM domain kinase 1 (LIMK1). PAK4 was also shown to mediate cell scaffold building activated by PKB/AKT1,²¹ activate nuclear factor κB (NF-κB)²² through binding to TNFR and TRADD²³, enhance the phosphorylation of LIMK1 by binding to DGCR6L²⁴, regulate gene translation through interactions with β-catenin,²⁵ and promote apoptosis via the SH3RF2²⁶ and Bcl-2 antagonist of

cell death (BAD).²⁷ Thus PAK4 is crucial in oncogenic transformation, cancer progression and invasion.²⁸ Increasing data have suggested that the aberrant expression of PAK4 is closely related to the progression and development of lung, ovarian, prostate, breast cancers, colon and gastric cancers, choriocarcinoma, and glioma^{17, 20} Therefore the targeting of PAK4 with small molecule inhibitors is one of the most promising new approaches to cancer treatment, and a number of programs to develop PAK4 inhibitors are currently in progress (Fig.1).¹¹

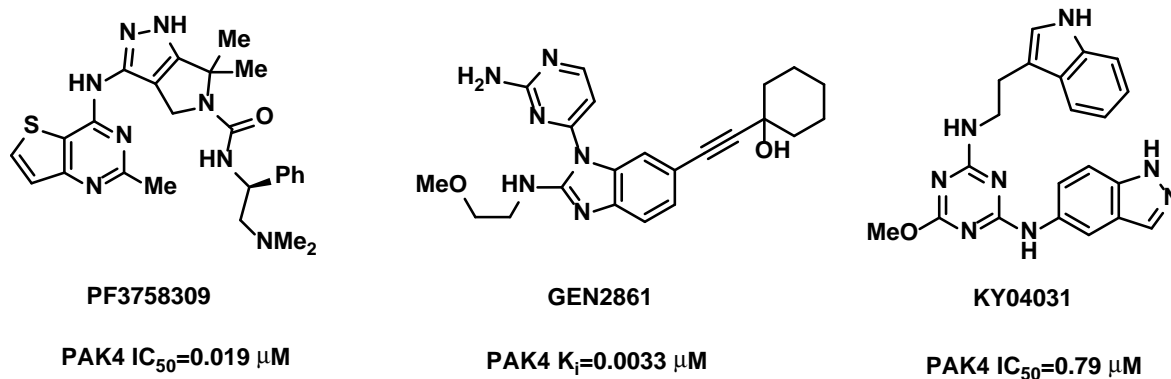


Fig. 1 Chemical structures of representative PAK4 inhibitors.

Recently, we launched a high throughput screening (HTS) campaign, which identified (-)-β-hydrastine²⁹ (1) and noscapine³⁰ (2) in Fig.2 as PAK4 inhibitors from our in-house natural products database. Followed by hit optimization, we found that a series of 1-phenanthryl-tetrahydroisoquinoline analogues, such as 3, were inhibitors of PAK4 with modest ability to attenuate the growth of cancer cells³⁰. To further develop better inhibitors based on this novel scaffold, we conducted an alternative structural modification to compound 3. Herein, we report the discovery of SSD-0501 (12a) which is shown to regulate the PAK4-LIMK1-Cofilin signal pathway, thereby inhibiting cellular invasion. In addition, the results show that this compound promotes apoptosis in A549 tumor cell *in vitro*, and inhibits A549 tumor xenograft growth *in vivo*.

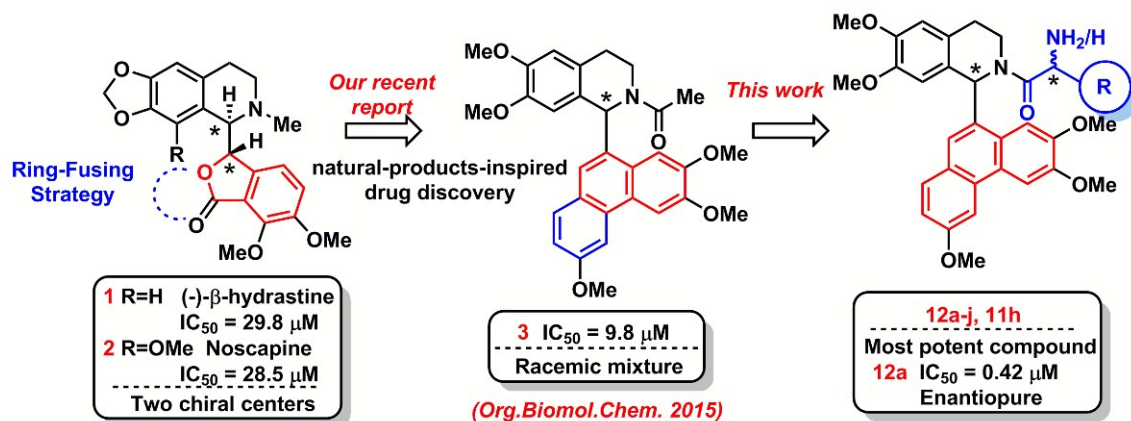
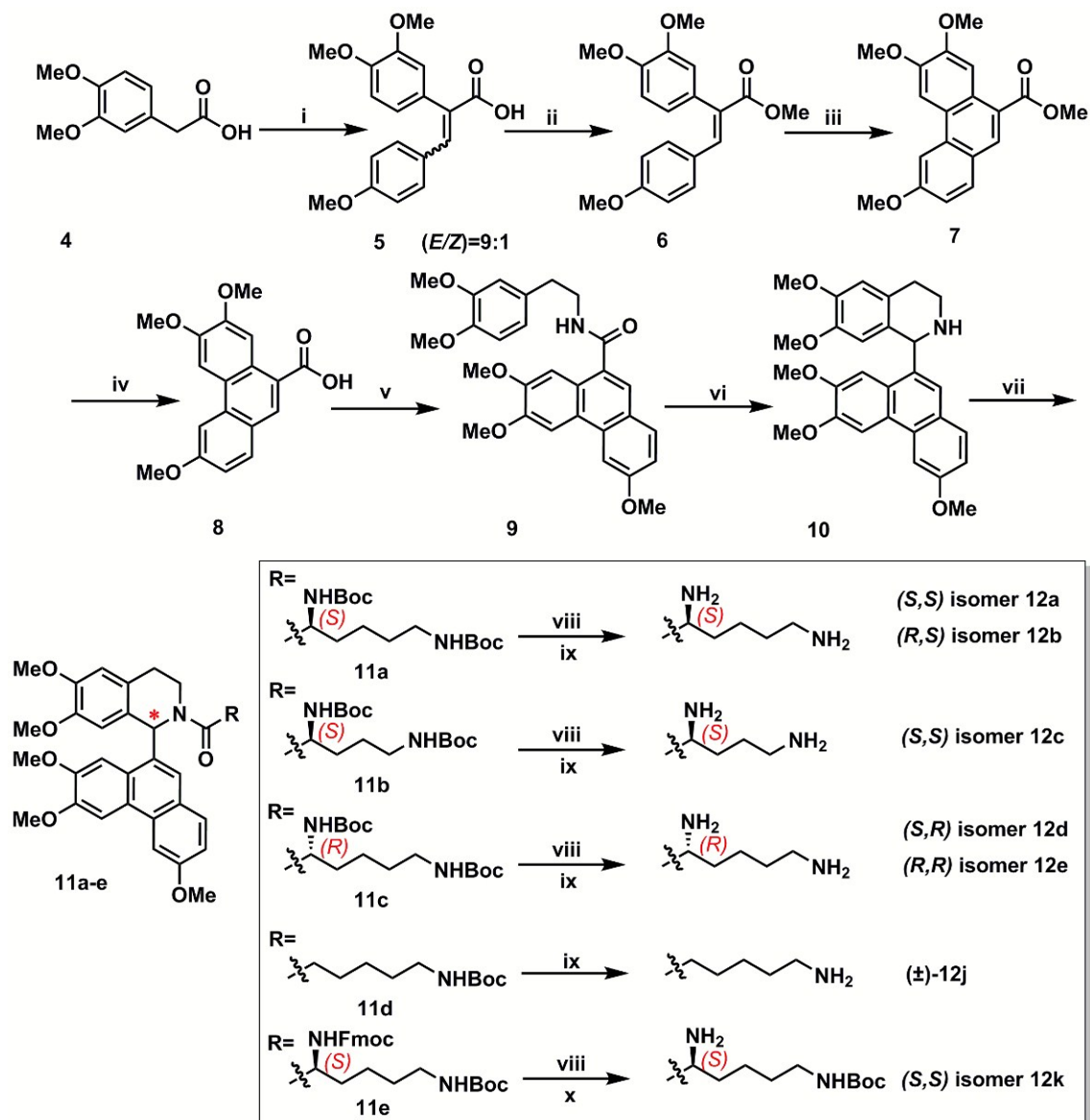


Fig. 2 Design of target molecules from 1(β-hydrastine) and 2(noscapine).

Chemistry

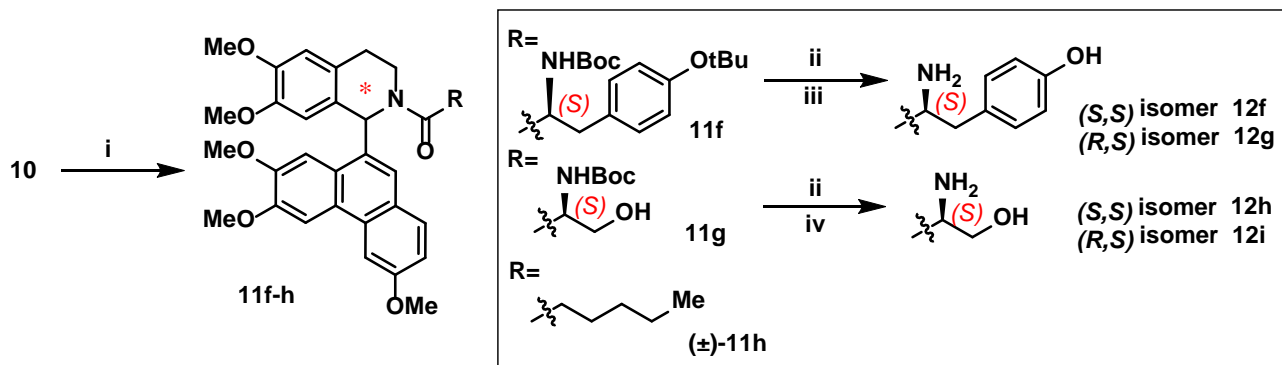
The syntheses of 1-phenanthryl-tetrahydroisoquinolin analogues (11h, 12a-j) are illustrated in Scheme 1 and 2. Condensation of 3, 4-dimethoxyphenyl acetic acid with anisic aldehyde in acetic anhydride provided 5 (*E/Z*=9:1). Methylation of *E*-5 afforded the corresponding methyl ester *E*-6, but *Z*-5 didn't react under this condition. The reaction mixture was purified to afford pure *E*-6. Intramolecular oxidative coupling of 6 with oxidant FeCl₃ gave the product 7 in 65% yield.³¹ The methyl ester 7 was hydrolyzed to the desired carboxylic acid 8 with sodium hydroxide in a high yield. Condensation of 3, 4-dimethoxyphenethylamine with 8 gave amide 9, which was followed by cyclization, reduction to afford 10. Standard peptide coupling conditions utilizing HATU furnished

amides **11a-11h**. At last, each compound was separated by silica gel column chromatography and the protecting groups were removed if necessary to afford the target molecules (**11h**, **12a-j**) (Table 1). The absolute stereochemistry of compounds **12a** and **12b** (diastereomers) were postulated via a comparison between the experimental and theoretical electronic circular dichroism (ECD) spectra³². The absolute configurations of the rest of analogs were assigned by comparing ECD spectra and specific rotations with **12a** and **12b**.



Scheme 1. Synthesis of Compounds (**12a-e**, **12j**, **12k**).

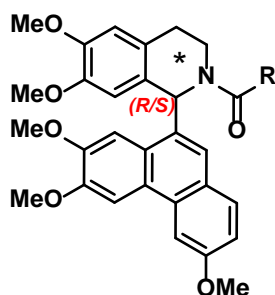
Reagents and conditions: (i) a) 4-methoxybenzaldehyde, Ac₂O, Et₃N, reflux, 10 h; b) NaOH (aq), 2 h; (ii) H₂SO₄, MeOH, reflux, 4 h; (iii) FeCl₃, DCM, 0 °C, 8 h; (iv) NaOH, MeOH, H₂O, reflux, 4 h; (v) a) EDCl, HOBt, DCM, 0 °C, 3 h; b) DIPEA, 3,4-dimethoxyphenethylamine, r.t., 0.5 h; (vi) a) POCl₃, DME, reflux, 2 h; b) NaBH₄, MeOH, 0 °C, 0.5 h; (vii) substituted acid, HATU, DCM, DIPEA, 0 °C, 0.5 h; (viii) diastereomers separation; (ix) HCl, ethyl acetate, r.t., 12 h; (x) diethylamine/CH₃CN, r.t., 2.5 h.



Scheme 2. Synthesis of Compounds (**11h**, **12f-12i**).

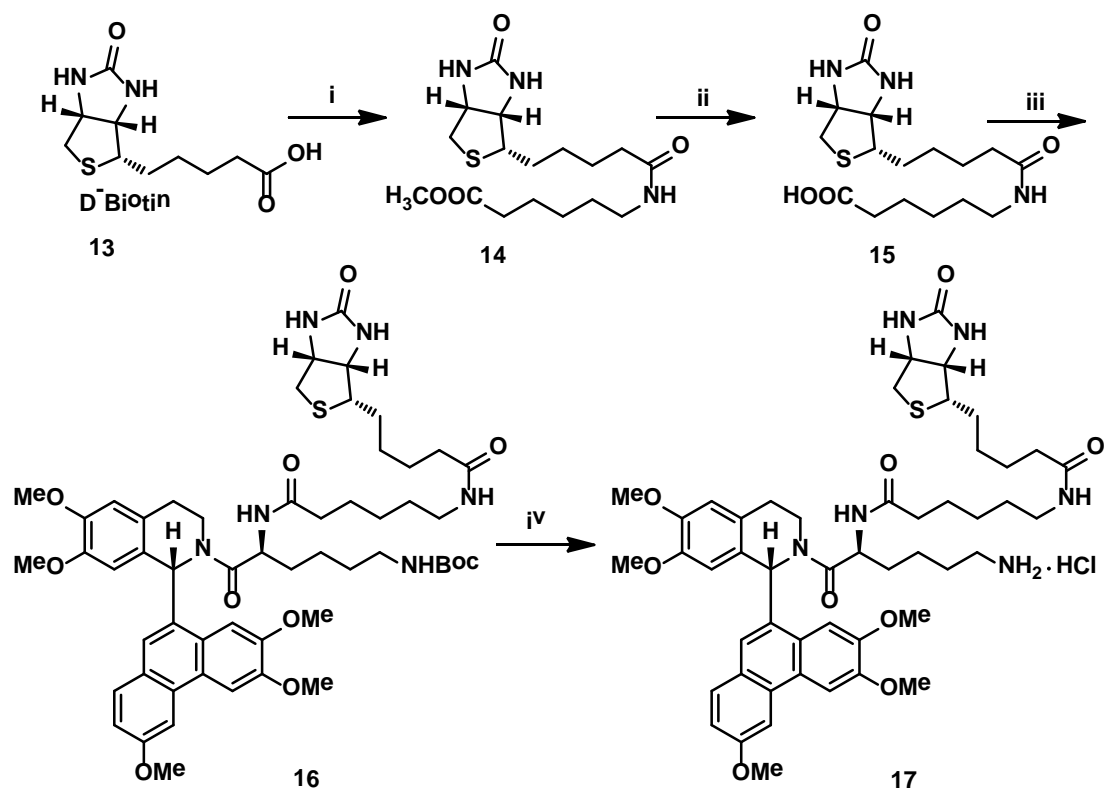
Reagents and conditions: (i) substituted acid, HATU, DCM, DIPEA, 0°C, 0.5 h; (ii) diastereomers separation; (iii) CF₃COOH/DCM, r.t., 0.5 h; (iv) HCl, ethyl acetate, r.t., 12 h.

Table 1. Structures of 1-phenanthrenyl-tetrahydroisoquinolin analogues



Compds	R	Compds	R	Compds	R
3	Me	(<i>S</i> *)- 12d		(<i>S</i> *)- 12h	
(<i>S</i> *)- 12a		(<i>R</i> *)- 12e		(<i>R</i> *)- 12i	
(<i>R</i> *)- 12b		(<i>S</i> *)- 12f		(±)- 12j	
(<i>S</i> *)- 12c		(<i>R</i> *)- 12g		(±)- 11h	

To further evaluate the binding mode of **12a** with PAK4, we have designed and synthesized biotinconjugated **12a** by attaching the biotin residue through a 6-aminohexanoic acid linking spacer to the free α -amino group. The biotinylation agent containing the spacer (**15**, Scheme 3) can be prepared from biotin and methyl 6-aminohexanoate hydrochloride as reported.³³ The coupling between **15** and **12k** was mediated by EDCI and HOBT. Finally, removal of the Boc group yielded the desired biotin-labeled **12a** in good yield.



Scheme 3. Reagents and conditions: (i) Methyl 6-aminohexanoate hydrochloride, EDCI, HOBt, DMF, TEA, r.t., 18 h; (ii) NaOH, THF, H₂O, r.t., 20 h; (iii) **12k**, EDCI, HOBT, DMF, DIPEA, r.t., 24 h; (iv) HCl, ethyl acetate, r.t., 4 h.

Results and discussion

Kinase assay

A kinase assay (Table 2) was performed to assess the potency of PAK4 inhibitors. With the moderate PAK4 inhibitor **3** as our lead, further optimization introduced a side chain including a hydrogen bond donor. When investigated for potency, compound **12a** exhibited the most potent inhibitory activity against PAK4, with an IC₅₀ value of 0.42 μM. Compared to **12a**, a slight loss in PAK4 affinity was observed for its diastereomer **12b**. Furthermore, inversion of the α-amino group is tolerated (**12a** versus **12d** and **12e**), whereas shortening the linker between isoquinoline and the end of the hydrogen bond donor led to the loss of inhibitory activity (**12a** versus **12c**, **12f-i**), suggesting that the length of the side chain plays a critical role in the inhibitory effects. In addition, we found that the terminal amino group was an important contributor to inhibitory activity, as removing the amino group from compound **12j** led to a more than 6-fold drop in potency (**11h**). These results suggest that PAK4 inhibitory activity is sensitive to the *N*-substituents. A summary of the *in vitro* SAR of the 1-phenanthryl-tetrahydroisoquinoline series of PAK4 inhibitors is presented in Fig.3.

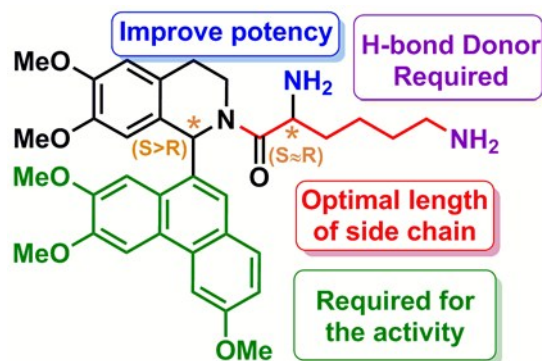


Fig. 3 *In vitro* SAR of 1-phenanthryl-tetrahydroisoquinoline series of PAK4 inhibitors.

Anti-proliferative assays

The anti-proliferative effects of the compounds in the PAK4-dependent tumor cell lines A549 (human lung epithelial cell) and MCF-7 (human breast cancer cell) are listed in Table 2. The tumor cell line HT-1080 (human fibrosarcoma cell), whose growth is not dependent on PAK4, was used to test the potential off-target effects of potent PAK4 inhibitors. In parallel with the enzymatic results, some compounds displayed high anti-proliferative effects in the PAK4-dependent tumor cell lines, especially A549. Compound **12a**, bearing a six-carbon chain with a primary amino group, showed an IC₅₀ value of 0.28 μM. Compound **12c** displayed a 30-fold lower cellular potency than compound **12a**, with an IC₅₀ value of 8.45 μM. Compound **12j**, without the α-amino group, was less potent than compound **12a** in the cellular assay, with an IC₅₀ value of 11.57 μM. Compounds **12b**, **12f**, and **12g** had shorter side chains and displayed weaker anti-proliferative effects.

Table 2 Kinase inhibitory potency against PAK4 and anti-proliferative effects against A549, MCF-7 and HT1080 cells of target compounds.

Compd.	PAK4(IC ₅₀ , μM)	IC ₅₀ (μM) ^a		
		A549	MCF-7	HT1080
12a	0.42 ± 0.01	0.28	0.83	15.89
12b	0.56 ± 0.02	0.37	1.28	14.06
12c	2.58 ± 0.009	8.45	5.17	>30
12d	0.52 ± 0.008	0.89	4.76	21.69
12e	0.64 ± 0.03	0.59	1.89	>30
12f	2.88 ± 0.13	1.55	2.33	27.29
12g	5.01 ± 0.09	3.78	3.16	>30
12h	4.22 ± 0.09	0.66	4.91	>30
12i	2.74 ± 0.02	0.22	0.72	3.71
12j	3.07 ± 0.021	11.57	3.88	>30
11h	19.87 ± 0.11	NT ^b	NT	NT
PF-3758309^c	0.019 ± 0.01	0.011	0.019	10.25

^a IC₅₀: Concentration of the compound (μM) producing 50% cell growth inhibition after 24 h of drug exposure, as determined by the MTT assay. Each experiment was carried out in triplicate. ^b NT: not tested in this assay. ^c Used as a positive control compound.

Compound **12a** Induce G₁/S Regulation and Apoptosis of A549 Cells

We next investigated the effects of the active compound on the cell cycle. Compound **12a** was chosen and evaluated using the A549 cancer cell line. A549 cells were treated with different concentrations of **12a** for 24 h, and the percentage of each cell cycle phase was calculated by the ratio of the population of cells with certain gated fluorescence intensity over the total counted cell number. The results are shown in Fig.4. An up-regulation in the G₁ phase of the cell cycle was observed in **12a**-treated (0.20 μM) A549 cells (Fig.4A and 4B). Western blot analysis revealed that compound **12a** markedly decreased levels of PAK4^{p-Ser474}, cyclins (e.g., cyclin D3), and CDKs (CDK2, CDK6) at the G₁/S transition to inhibit the proliferation of tumor cells (Fig.4C).

To assess whether the active compound could induce cancer cell apoptosis, **12a**-treated A549 cells were analyzed. The data (Fig.5A and 5B) revealed a concentration-dependent, high level of activity that stimulated early cell apoptosis at 0.2 μM and 1.0 μM. Compound **12a** was also found to down-regulate the expression level of Bcl-2 and up-regulate the expression level of Bax, caspase 3, and caspase 8 (Fig.5C). These results confirmed that compound **12a** efficiently induced early apoptosis in A549 cells.

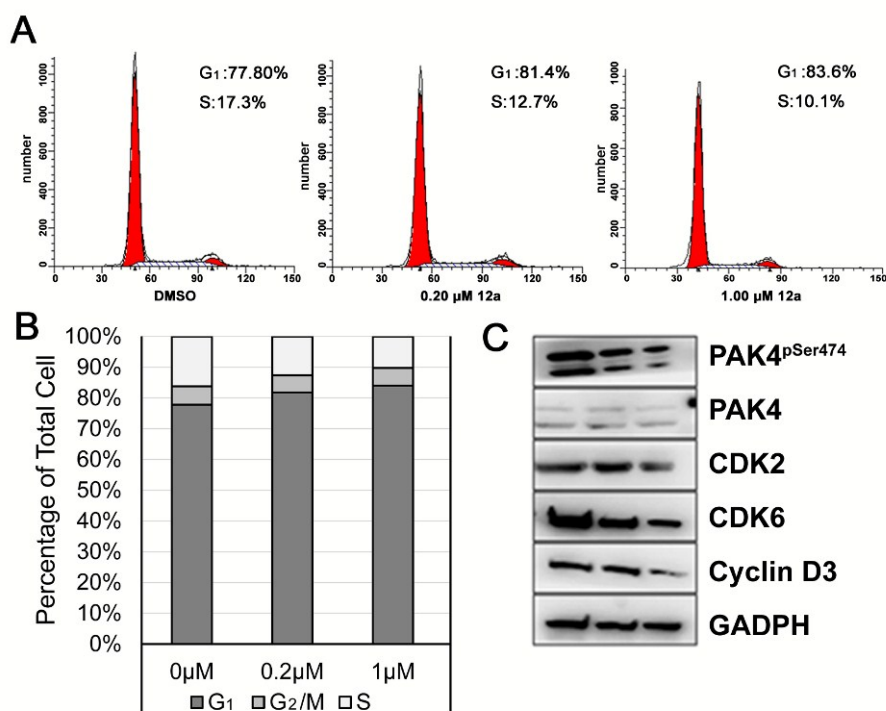


Fig. 4 Compound **12a** affects the cell cycle distribution in A549 cancer cells. (A) A549 cells were pre-incubated with **12a** at different concentrations for 24 h, and then the cells were analyzed using a FACS Vantage flow cytometer with the Cell Quest acquisition and analysis software program. The experiment was repeated 3 times. One representative experiment is shown; (B) The statistical graph of cell cycle distribution; (C) Proteins of the cells indicated in A were extracted to examine the expression of the indicated proteins by western blot analysis. The membrane was sequentially probed with the indicated antibodies. **12a** down-regulates the expression level of PAK4^{pSer474}, Cyclin D3 and CDK2/6.

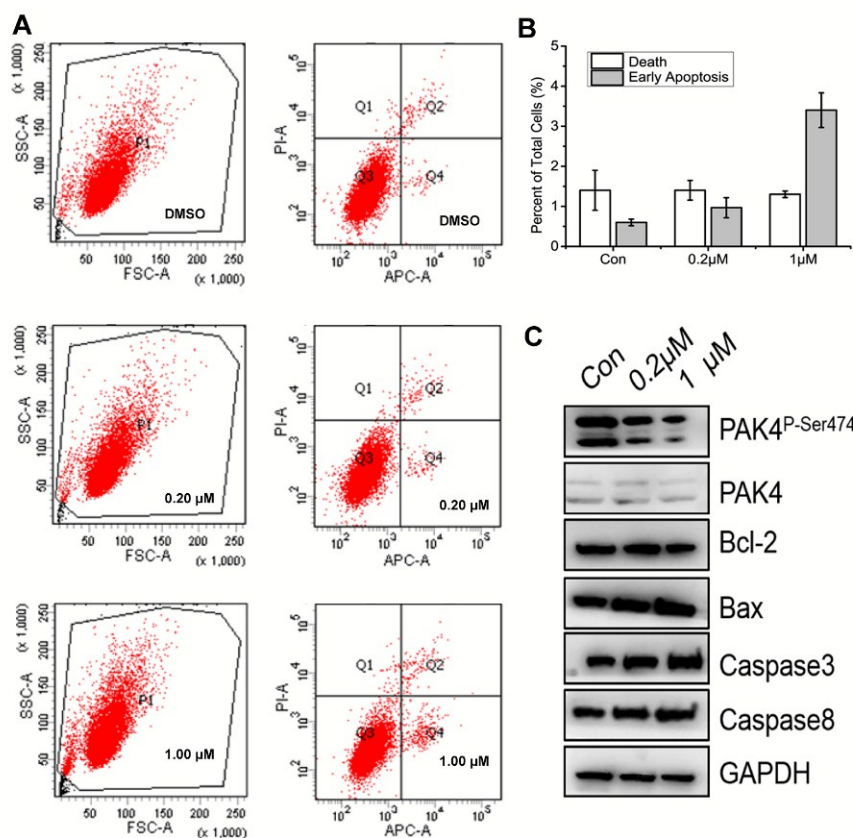


Fig. 5 The effect of **12a** on apoptosis of A549 cancer cells. (A) A549 cells were pre-incubated with **12a** at different concentrations for 24 h, and then the cells were treated using the Annexin V-FITC apoptosis detection kit and analyzed with FACS. The experiment was repeated 3 times. One representative experiment is shown; (B) The statistical graph of early apoptosis distribution; (C) A549 cells were treated with **12a** for 24 h and then examined for expression of indicated proteins by western blot analysis. **12a** down-regulates the Bcl-2 expression and up-regulates BAX, Caspase 3, and Caspase 8.

Compound **12a** inhibited the invasive potential of A549 cells and downstream signaling pathways

As previously mentioned, PAK4 has been closely associated with the migration and invasion of tumors. From the results described above, compound **12a** stood out with high potency against both PAK4 kinase and tumor cells. This compound was further evaluated in a Transwell assay at indicated concentrations to examine the effect on these characteristics in the NCI-H446 (human small cell lung cancer cell), A549, MCF-7, and MDA-MB-231 (human breast cancer cell) cell lines. As shown in Fig.6A and 6B, in A549, MCF-7 and MDA-MB-231 cells, a dose-dependent decrease in cell invasiveness was observed following treatment with compound **12a**.

Previous work showed that the PAK4/LIMK1/Cofilin signaling pathway is correlated with cellular invasive behavior. We therefore investigated the effects of compound **12a** on the PAK4/LIMK1/Cofilin signaling pathway by Western blot analysis. As expected, in A549 cells treated with different concentrations of compound **12a** for 24 h, we observed inhibition of LIMK1 and Cofilin phosphorylation in a dose-dependent manner (Fig.6C).

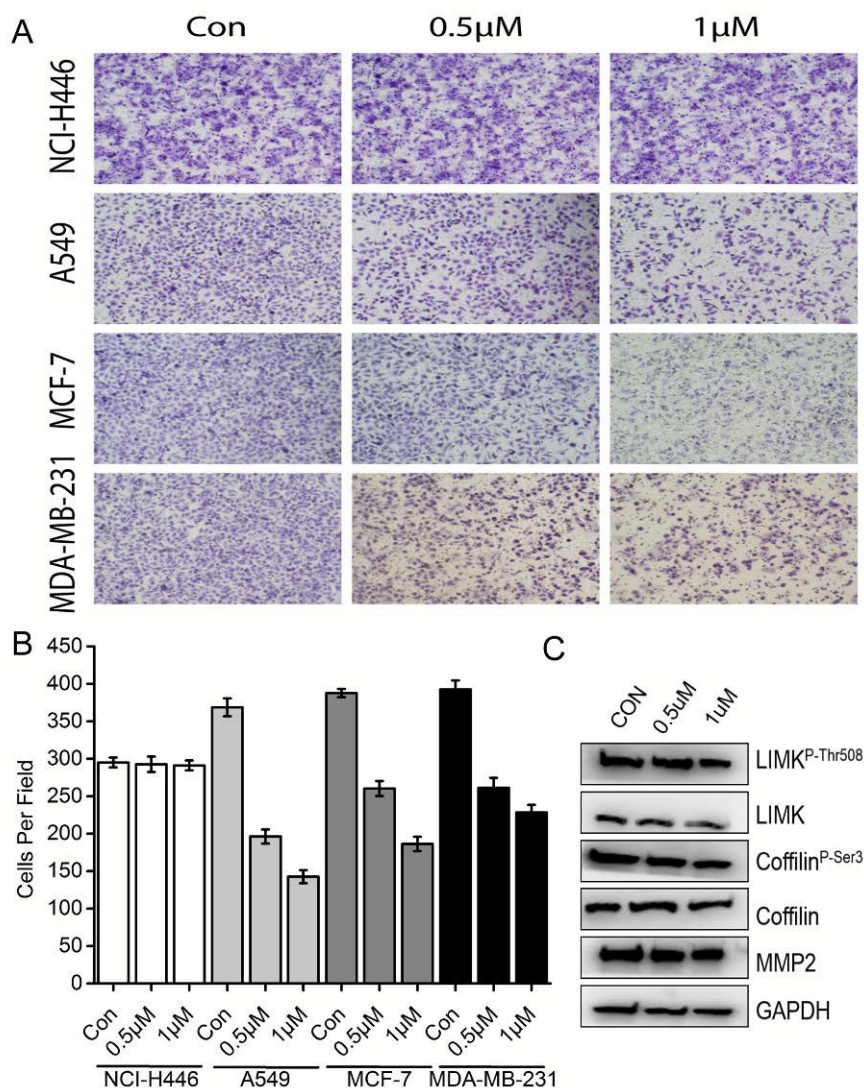


Fig. 6 **12a** suppresses invasion of A549 cancer cells and inhibits PAK4/LIMK1/cofilin pathway (A) NCI-H446, A549, MCF-7, and MDA-MB-231 cells invasive capacity was evaluated by using a Boyden chamber matrigel invasion assay. After 24 h of indicated concentrations of **12a** treatment, the invaded cells were fixed and stained, and 10 random fields were counted; (B) The statistical graph of invasive cells distribution; (C) The expression levels of LIMK1/LIMK1^{p-Thr508}, cofilin/cofilin^{p-Ser3}, MMP2 in A549 cells.

Lentiviral-vector mediated small interfering RNA (siRNA) knockdown of PAK4

To further analyze the invasiveness stimulated by PAK4, A549 cells were infected with Lentiviral pSR α -HA-PAK4 (wild-type PAK4, PAK4^{WT}) and pSR α -HA-PAK4M350 (kinase dead PAK4, PAK4^{KM}). At a concentration of 0.5 μ M, PAK4^{WT}, but not PAK4^{KM}, enhanced the inhibitory effect of **12a** on the invasion of A549 cells. Furthermore, opposite results were obtained following the silencing of PAK4 in the A549 cells. These results clearly suggest that treatment of **12a**, by targeting PAK4, exhibits anti-invasive effects in human pulmonary carcinoma cells (Fig.7).

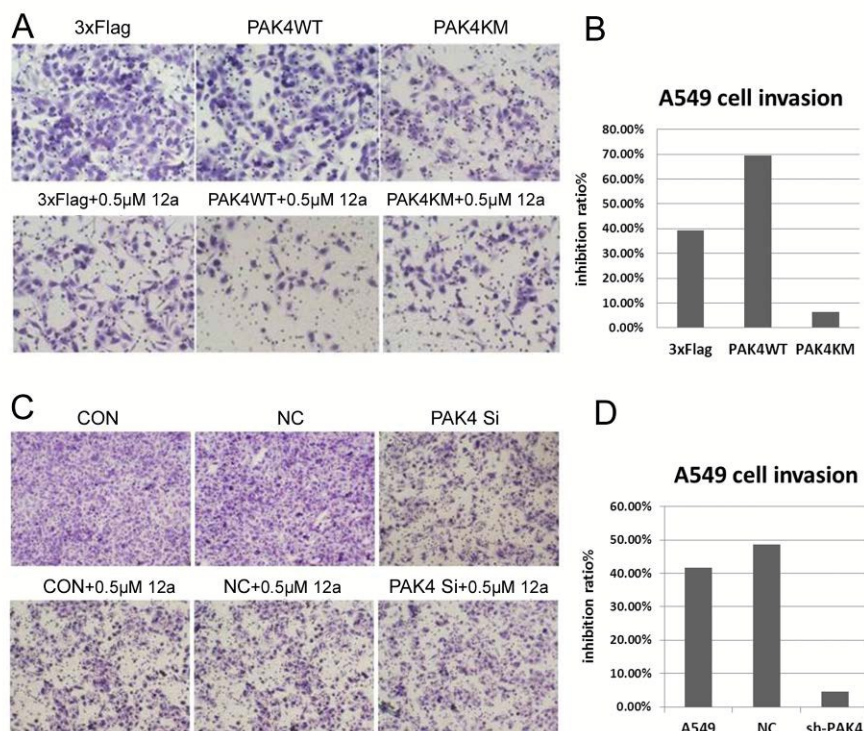


Fig. 7 **12a** inhibits the invasive potential of A549 cells via inhibition of PAK4 kinase activity. (A) PAK4^{WT} and PAK4^{KM} A549 cells invasive capacity was evaluated by using a Boyden chamber matrigel invasion assay. A549 cells were transfected with pCDNA3.1-3×Flag, pCDNA3.1-3×Flag-PAK4^{WT} or pCDNA3.1-3×Flag-PAK4^{KM}, and the Transwell assay was performed after treatment with 0.5 μM of **12a**. The experiment was repeated 3 independent times. (B) The statistical graph of invasive cells distribution; (C) PAK4^{Si} A549 invasive capacities were evaluated. A549 cells stably transfected with shPAK4 were used for the Transwell assay. The experiment was repeated three independent times; (D) The statistical graph of invasive cells distribution.

Immunoprecipitation assay

Considering its unique scaffold from other known PAK4 inhibitors, biotin-streptavidin system was used to detect the combination mode between **12a** and PAK4. Flag-PAK4 (full-length protein), Flag-PAK4 (1-325aa) or Flag-PAK4 (326-592aa) was transfected into A549 cells and incubated with biotin-labeled **12a** for 12 h. The total cell lysate was immunoprecipitated with sepharose beads (streptavidin conjugate) and then detected by Western blot assay with α-Flag antibody. We found that the biotin-labeled **12a** could bind both the N and C termini of PAK4 in the concentration 0.50 μM (Fig.8).

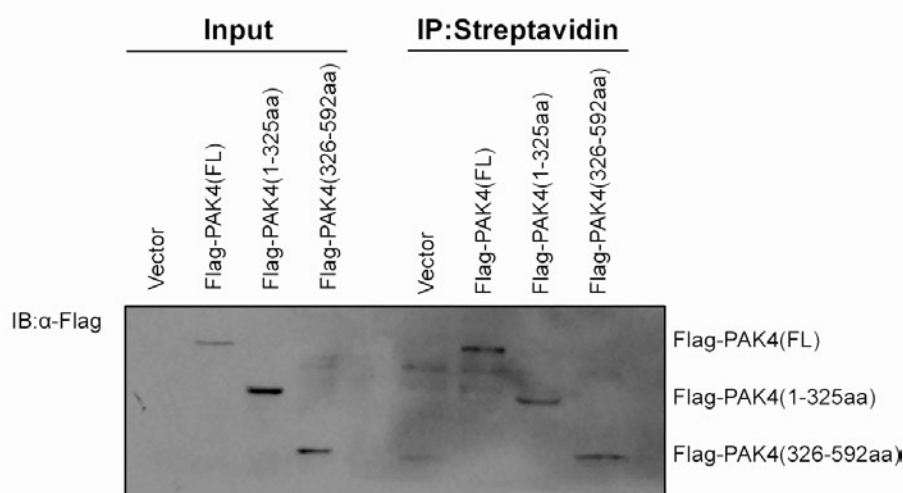


Fig.8 12a (Biotin conjugate) binds to PAK4 N-terminal (1-325aa) and C-terminal (326aa-592aa). Flag-PAK4 (FL), Flag-PAK4 (1-325aa) or Flag-PAK4 (326-592aa) was transfected into A549 cells respectively and then incubated with **12a** (biotin conjugate) for 12 hr. Total cell lysate was immunoprecipitated with sepharose beads (streptavidin conjugate), and then detected by western blot assay with α -Flag antibody.

In Vivo Antitumor Efficacy Study

To evaluate the effect of this compound against tumor growth *in vivo*, we performed A549 xenograft human lung cancer cell mouse model tumor formation experiments (Fig.9). Compound **12a** was administered orally with 0.5% CMC-Na (sodium carboxymethyl cellulose) at doses of 50, 20 and 8 mg/kg once daily for 14 consecutive days. Compared with vehicle treatment, compound **12a** significantly inhibited tumor growth at 50 mg/kg, with tumor growth inhibitory rates >55% ($p < 0.05$) and no significant body weight loss.

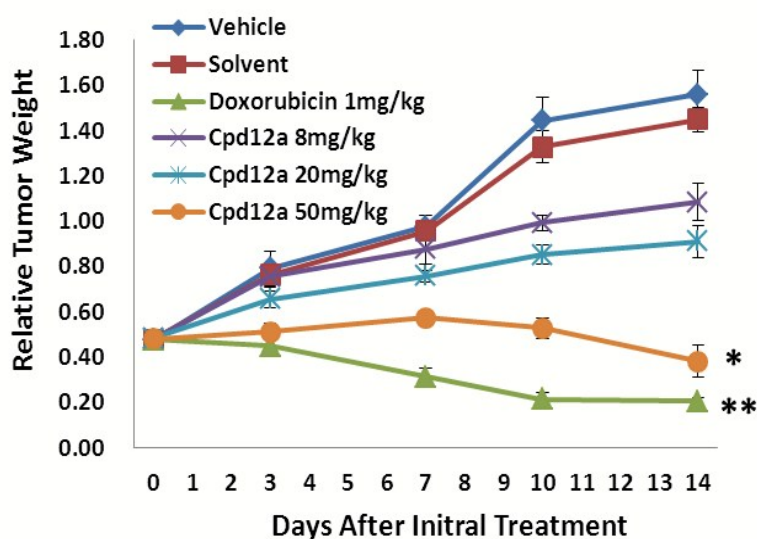


Fig.9 Antitumor activity of **12a** in A549 xenograft model. Mice bearing A549 were orally administered compound **12a** and Doxorubicin (* $P < 0.05$, ** $P < 0.01$).

Experimental

Chemistry

$^1\text{H-NMR}$ and $^{13}\text{C-NMR}$ spectral data were recorded in CDCl_3 or $\text{DMSO-}d_6$ on Bruker ARX-400 NMR or Bruker ARX-600 NMR spectrometer. High resolution accurate mass determinations (HRMS) for all final target compounds were obtained on a Bruker Micromass Time of Flight mass spectrometer equipped with electrospray ionisation (ESI). Unless otherwise noted, all commercial reagents and solvents were purchased from vendors and were used without further purification or distillation. The purities of compounds used for biological evaluation were determined on a Waters 2000 HPLC system: column, Unitary C18, 4.6 mm \times 250 mm, 5 μm . HPLC conditions A (for compound **11h**): solvent A = H_2O , solvent B = MeOH; flow rate = 1.0 mL/min; compounds were eluted with a gradient of 75% MeOH/ H_2O to 95% MeOH/ H_2O for 15 min. HPLC conditions B (for compound **12a** to **12j**): solvent A = H_2O containing 0.1% trifluoroacetic acid (TFA), solvent B = MeCN; flow rate = 1.0 mL/min; compounds were eluted with a gradient of 20% MeCN/ H_2O to 95% MeCN/ H_2O for 15 min. Purity was determined by total absorbance at 254 nm. The purity of each inhibitor was determined to be >95%. Column chromatography was carried out on silica gel (200–300 mesh). All reactions were monitored using thin layer chromatography (TLC) on silica gel plates. Optical rotation: MCP 200 Modular Circular Polarimeter (Anton Paar); concentration c in g per 100 mL; $T = 20\text{ }^\circ\text{C}$; wavelength 589 nm (D-line of Na light); the unit of the specific rotation ($[\alpha]_D^{25}$ grad mL dm^{-1} g^{-1}) is omitted for clarity.

General Procedure for the Synthesis of compounds 11a-h.

The key intermediate **10** was synthesized using a convenient six-step procedure starting from (3,4-dimethoxyphenyl)acetic acid as shown in Scheme 1, which was illustrated in detail in the supplementary information. To a mixture of **10** (459 mg, 1 mmol), substituted acid (1 mmol), and diisopropylethylamine (0.33 mL, 2 mmol) in dichloromethane (15 mL), *O*-(7-Azabenzotriazol-1-yl)-*N,N,N,N*-tetramethyluronium hexafluorophosphate (HATU) (380 mg, 1 mmol) was added portion-wise over 10 min. The mixture was stirred at 0 °C for 1 h. The organic solution was washed with water, dried with MgSO₄. Removal of the solvent gave a residue, which was purified by column chromatography (silica gel, CH₂Cl₂/acetone=20:1 as eluent) to afford product **11a-h** in quantitative yield. The mixture of diastereomers (**11a-c**, **11e-g**) were separated into the individual components.

1-(6,7-dimethoxy-1-(3,6,7-trimethoxyphenanthren-9-yl)-3,4-dihydroisoquinolin-2(1H)-yl)hexan-1-one (11h)

White solid, yield 90.9%. HPLC: 97.38 %, t_R = 13.202 min. ¹H NMR (600MHz, CDCl₃) δ 8.22 (s, 1H), 7.92 (s, 1H), 7.84 (d, J = 2.16 Hz, 1H), 7.56 (d, J = 8.76 Hz, 1H), 7.43 (s, 1H), 7.12 (dd, J = 8.76, 2.34 Hz, 1H), 6.87 (s, 1H), 6.72 (s, 1H), 6.59 (s, 1H), 4.12 (s, 6H), 4.00 (s, 3H), 3.94 (s, 3H), 3.73 (s, 3H), 3.70-3.66 (m, 1H), 3.48-3.42 (m, 1H), 3.04-3.01 (m, 1H), 2.82-2.78 (m, 1H), 2.47-2.42 (m, 1H), 2.37-2.31 (m, 1H), 1.67-1.61 (m, 2H), 1.30-1.25 (m, 4H), 0.85 (t, J = 6.9 Hz, 3H). ¹³C NMR (150MHz, CDCl₃) δ 171.8, 158.5, 149.8, 148.9, 148.2, 147.6, 133.5, 131.0, 131.5, 128.4, 128.0, 126.8, 126.5, 125.1, 124.5, 115.2, 111.5, 111.1, 14.0, 106.3, 103.8, 103.5, 56.6, 56.0, 55.9, 55.9, 55.6, 52.8, 38.8, 33.5, 31.7, 28.6, 25.3, 22.5. HRMS calcd for C₃₄H₃₉NO₆Na [M+Na]⁺, 580.2670; found 580.2689.

(*S*)-2,6-diamino-1-((*S*)-6,7-dimethoxy-1-(3,6,7-trimethoxyphenanthren-9-yl)-3,4-dihydroisoquinolin-2(1H)-yl)hexan-1-one (12a)

To a mixture of (*S*, *S*)-**11a** (236 mg, 0.3 mmol) in ethyl acetate (15 mL) was dropwise added 2M HCl solution in ethyl acetate (15 mL). The resulting clear solution was stirred at room temperature for 12 h. The solid product was collected by filtration, washed with hexane, and dried under vacuum at 45°C for 24 h to give the hydrochloride salt of **12a**. White solid, yield 34.3% (two steps). HPLC: 96.96 %, t_R = 12.72 min. ¹H NMR (400MHz, DMSO-*d*₆) δ 8.39 (s, 3H), 8.14 (s, 1H), 8.08 (d, J = 1.64 Hz, 1H), 7.94 (s, 4H), 7.65 (d, J = 8.84 Hz, 1H), 7.34 (s, 1H), 7.15 (dd, J = 8.72, 2.08 Hz, 1H), 6.92 (s, 2H), 6.90 (s, 1H), 6.74 (s, 1H), 4.42-4.40 (m, 1H), 4.06 (s, 3H), 4.05 (s, 3H), 3.98 (s, 6H), 3.86-3.77 (s, 4H), 3.60 (s, 3H), 3.34-3.26 (m, 1H), 3.17-3.07 (m, 1H), 2.85-2.81 (m, 1H), 2.44-2.34 (s, 2H), 1.68-1.60 (m, 1H), 1.56-1.50 (m, 2H), 1.31-1.29 (m, 2H), 1.19-1.16 (m, 2H). ¹³C NMR (100MHz, DMSO-*d*₆) δ 168.5, 159.0, 149.9, 149.4, 148.7, 147.9, 133.0, 131.1, 130.9, 128.3, 127.3, 127.0, 126.2, 124.9, 124.8, 116.3, 112.2, 112.0, 105.9, 105.2, 104.6, 56.5, 56.3, 56.1 (2C), 56.0, 53.2, 50.1, 38.3, 30.9, 28.7, 26.6, 21.5, 21.0. HRMS calcd for C₃₄H₄₂N₃O₆ [M+H]⁺, 588.3068; found 588.3063. Specific rotation: $[\alpha]_D^{20}$ -115.7 (c = 1.00; MeOH).

(*S*)-2,6-diamino-1-((*R*)-6,7-dimethoxy-1-(3,6,7-trimethoxyphenanthren-9-yl)-3,4-dihydroisoquinolin-2(1H)-yl)hexan-1-one (12b)

Compound **12b** was prepared in a manner similar to that for **12a** in 36.5% yield (two steps). White solid. HPLC: 98.78 %, t_R = 9.442 min. ¹H NMR (400MHz, DMSO-*d*₆) δ 8.43 (s, 3H), 8.25 (s, 3H), 8.23 (s, 1H), 8.14 (s, 1H), 8.07 (s, 1H), 7.64 (d, J = 8.80 Hz, 1H), 7.35 (s, 1H), 7.13 (d, J = 8.64 Hz, 1H), 6.92 (s, 2H), 6.68 (s, 1H), 4.49 (s, 1H), 4.06-3.99 (m, 2H), 4.05 (s, 3H), 4.03 (s, 3H), 4.02 (s, 3H), 4.00 (s, 3H), 3.98 (s, 3H), 3.83 (s, 3H), 3.58 (s, 3H), 3.01 (s, 2H), 2.70 (s, 2H), 1.80 (s, 2H), 1.62 (s, 2H), 1.56-1.49 (m, 1H), 1.34 (s, 1H). ¹³C NMR (100MHz, DMSO-*d*₆) δ 167.5, 158.9, 150.1, 149.9, 148.6, 147.9, 132.5, 131.2, 130.9, 128.5, 127.8, 126.5, 126.4, 124.7, 124.7, 116.3, 112.1, 111.6, 106.7, 104.9, 104.4, 56.5, 56.2, 56.1, 56.0, 55.9, 53.2, 50.1, 38.5, 38.0, 30.6, 28.4, 26.7, 21.2. HRMS calcd for C₃₄H₄₂N₃O₆ [M+H]⁺, 588.3068; found 588.3071. Specific rotation: $[\alpha]_D^{20}$ 20.7 (c = 1.00; MeOH).

(*S*)-2,5-diamino-1-((*S*)-6,7-dimethoxy-1-(3,6,7-trimethoxyphenanthren-9-yl)-3,4-dihydroisoquinolin-2(1H)-yl)pentan-1-one (12c)

Compound **12c** was prepared in a manner similar to that for **12a** in 26.7% yield (two steps). White solid. HPLC: 97.80 %, $t_R = 4.712$ min. ^1H NMR (400 MHz, CDCl_3) δ 8.41 (s, 3H), 8.13 (s, 1H), 8.06 (d, $J = 2.00$ Hz, 1H), 7.96 (s, 3H), 7.93 (s, 1H), 7.65 (d, $J = 8.88$ Hz, 1H), 7.32 (s, 1H), 7.14 (dd, $J = 8.76, 2.28$ Hz, 1H), 6.92 (s, 1H), 6.91 (s, 1H), 6.70 (s, 1H), 4.40 (s, 1H), 4.04 (s, 3H), 3.98 (s, 3H), 3.96 (s, 3H), 3.82 (s, 3H), 3.80-3.75 (m, 1H), 3.59 (s, 3H), 3.40-3.36 (m, 1H), 3.18-3.09 (m, 1H), 2.87-2.82 (m, 1H), 2.65 (s, 2H), 1.65-1.58 (m, 4H). ^{13}C NMR (100 MHz, $\text{DMSO}-d_6$) δ 168.7, 158.9, 150.1, 149.4, 148.7, 147.9, 133.0, 131.2, 130.9, 128.3, 127.4, 127.2, 126.4, 124.9, 124.9, 116.3, 112.2, 112.0, 105.7, 105.1, 104.6, 56.5, 56.4, 56.1, 56.0 (2C), 53.3, 50.2, 39.1, 38.0, 28.9, 28.5, 23.0. HRMS calcd for $\text{C}_{33}\text{H}_{40}\text{N}_3\text{O}_6$ $[\text{M}+\text{H}]^+$, 574.2912; found 574.2931. Specific rotation: $[\alpha]_D^{20} -137.0$ ($c = 1.00$; MeOH).

(R)-2,6-diamino-1-((S)-6,7-dimethoxy-1-(3,6,7-trimethoxyphenanthren-9-yl)-3,4-dihydroisoquinolin-2(1H)-yl)hexan-1-one (12d)

Compound **12d** was prepared in a manner similar to that for **12a** in 29.7% yield (two steps). White solid. HPLC: 98.18 %, $t_R = 4.370$ min. ^1H NMR (400 MHz, $\text{DMSO}-d_6$) δ 8.42 (s, 3H), 8.14 (s, 1H), 8.08 (d, $J = 2.00$ Hz, 1H), 8.00 (s, 3H), 7.95 (s, 1H), 7.64 (d, $J = 8.88$ Hz, 1H), 7.35 (s, 1H), 7.15 (dd, $J = 8.76, 2.24$ Hz, 1H), 6.91 (d, $J = 9.48$ Hz, 2H), 6.74 (s, 1H), 4.41 (s, 1H), 4.06 (s, 3H), 3.99 (s, 6H), 3.82 (s, 3H), 3.79 (s, 1H), 3.60 (s, 3H), 3.30-3.27 (m, 1H), 3.18-3.09 (m, 1H), 2.85-2.80 (s, 1H), 2.42-2.37 (m, 2H), 1.69-1.67 (m, 1H), 1.58-1.50 (m, 1H), 1.32 (s, 2H), 1.25-1.16 (m, 2H). ^{13}C NMR (100 MHz, $\text{DMSO}-d_6$) δ 168.4, 159.0, 149.9, 149.4, 148.7, 147.9, 133.1 (2C), 131.2, 130.9, 128.3, 127.4, 127.0, 126.2, 124.9 (2C), 124.8, 116.3, 112.2, 112.0, 105.9, 105.2, 104.6, 56.5, 56.4, 56.1, 56.0, 53.1, 50.1, 38.3, 30.9, 28.9, 26.6, 21.0. HRMS calcd for $\text{C}_{34}\text{H}_{42}\text{N}_3\text{O}_6$ $[\text{M}+\text{H}]^+$, 588.3068; found 588.3074. Specific rotation: $[\alpha]_D^{20} -153.0$ ($c = 1.00$; MeOH).

(R)-2,6-diamino-1-((R)-6,7-dimethoxy-1-(3,6,7-trimethoxyphenanthren-9-yl)-3,4-dihydroisoquinolin-2(1H)-yl)hexan-1-one (12e)

Compound **12e** was prepared in a manner similar to that for **12a** in 33.4% yield (two steps). White solid. HPLC: 97.37 %, $t_R = 4.668$ min. ^1H NMR (400 MHz, $\text{DMSO}-d_6$) δ 8.39 (s, 3H), 8.23 (s, 1H), 8.17 (s, 3H), 8.14 (s, 1H), 8.07 (d, $J = 1.96$ Hz, 1H), 7.64 (d, $J = 8.84$ Hz, 1H), 7.35 (s, 1H), 7.14 (dd, $J = 8.72, 2.24$ Hz, 1H), 6.92 (s, 2H), 6.67 (s, 1H), 4.48 (s, 1H), 4.06 (s, 3H), 4.04 (s, 3H), 3.98 (s, 6H), 4.05-3.96 (m, 1H), 3.83 (s, 1H), 3.58 (s, 3H), 3.48-3.39 (m, 1H), 3.00-2.99 (m, 2H), 2.69 (s, 2H), 1.80-1.78 (m, 2H), 1.60-1.59 (m, 2H), 1.54-1.45 (s, 1H), 1.35-1.30 (m, 1H). ^{13}C NMR (100 MHz, $\text{DMSO}-d_6$) δ 167.5, 158.9, 150.1, 149.4, 148.6, 147.9, 132.5, 131.2 (2C), 130.9, 128.5, 127.8, 126.5, 126.4, 124.7, 124.7 (2C), 116.3, 112.1, 111.6, 106.7, 104.9, 104.4, 56.5, 56.2, 56.1, 56.0, 55.9, 53.2, 50.1, 38.5, 30.6, 26.7, 21.3. HRMS calcd for $\text{C}_{34}\text{H}_{42}\text{N}_3\text{O}_6$ $[\text{M}+\text{H}]^+$, 588.3068; found 588.3066. Specific rotation: $[\alpha]_D^{20} 43.7$ ($c = 1.00$; MeOH).

(S)-2-amino-1-((S)-6,7-dimethoxy-1-(3,6,7-trimethoxyphenanthren-9-yl)-3,4-dihydroisoquinolin-2(1H)-yl)-3-(4-hydroxyphenyl)propan-1-one (12f)

To a solution of (*S, S*)-**11f** (233 mg, 0.3 mmol) in CH_2Cl_2 (3.5 mL) was dropwise added TFA (1.5 mL). The mixture was stirred at room temperature for 0.5 h. The solvent was evaporated and the residue was purified by column chromatography (silica gel, $\text{CH}_2\text{Cl}_2/\text{MeOH}=20:1$) to give compound **12f** in 24.9% yield (two steps). White solid. HPLC: 98.28 %, $t_R = 5.620$ min. ^1H NMR (400 MHz, $\text{DMSO}-d_6$) δ 9.40 (s, 1H), 8.23 (s, 1H), 8.13-8.05 (m, 4H), 7.60 (d, $J = 8.84$ Hz, 1H), 7.33 (s, 1H), 7.12 (dd, $J = 8.80, 2.32$ Hz, 1H), 6.87 (d, $J = 8.44$ Hz, 2H), 6.85 (s, 1H), 6.64 (d, $J = 10.56$ Hz, 2H), 6.51 (d, $J = 8.44$ Hz, 2H), 4.60-4.56 (m, 1H), 4.04 (m, 3H), 4.00 (m, 3H), 3.97 (s, 1H), 3.95-3.89 (m, 1H), 3.83 (s, 1H), 3.60 (s, 3H), 3.43-3.41 (m, 1H), 3.30-3.26 (m, 1H), 3.02-2.92 (m, 2H), 2.68-2.63 (m, 1H). ^{13}C NMR (100 MHz, $\text{DMSO}-d_6$) δ 167.4, 158.3, 156.7, 149.1, 148.0, 147.2, 132.1, 130.8, 130.6 (2C), 128.4, 126.9, 126.5, 126.2, 124.4, 124.3, 124.3, 115.9, 115.6 (2C), 111.6, 110.9, 106.4, 104.5, 104.1, 56.1, 55.9, 55.7, 55.5, 55.3, 53.1, 50.7, 38.0, 36.9, 27.3. HRMS calcd for $\text{C}_{37}\text{H}_{39}\text{N}_2\text{O}_7$ $[\text{M}+\text{Na}]^+$, 623.2752; found 623.2756. Specific rotation: $[\alpha]_D^{20} -64.3$ ($c = 1.00$; MeOH).

(S)-2-amino-1-((R)-6,7-dimethoxy-1-(3,6,7-trimethoxyphenanthren-9-yl)-3,4-dihydroisoquinolin-2(1H)-yl)-3-

4-hydroxyphenyl)propan-1-one (12g)

Compound **12g** was prepared in a manner similar to that for **12f** in 28.9% yield (two steps). White solid. HPLC: 95.72 %, $t_R = 5.717$ min. $^1\text{H NMR}$ (400 MHz, $\text{DMSO-}d_6$) δ 9.01 (s, 1H), 8.21 (s, 1H), 8.15 (s, 1H), 8.10 (d, $J = 2.04$ Hz, 1H), 7.61 (d, $J = 8.84$ Hz, 1H), 7.37 (s, 1H), 7.13 (dd, $J = 8.76, 2.32$ Hz, 1H), 6.85 (s, 1H), 6.79 (d, $J = 8.44$ Hz, 2H), 6.67 (s, 1H), 6.33 (d, $J = 8.44$ Hz, 2H), 4.06 (m, 3H), 3.99 (m, 3H), 3.98 (s, 1H), 3.80-3.78 (m, 4H), 3.60 (s, 3H), 3.56-3.55 (m, 1H), 3.16-3.00 (m, 2H), 2.76-2.72 (m, 1H), 2.55-2.54 (m, 1H), 2.48-2.42 (m, 1H), 1.75 (s, 2H). $^{13}\text{C NMR}$ (100 MHz, $\text{DMSO-}d_6$) δ 174.3, 158.8, 155.9, 149.9, 149.3, 148.4, 147.7, 133.7, 130.8, 130.6 (2C), 128.4, 128.0, 127.8, 127.5, 126.7, 124.8 (2C), 116.2, 115.1 (2C), 112.2, 111.9, 106.5, 105.0, 104.5, 56.4, 56.1, 56.0, 55.9, 53.2, 53.0, 42.3, 38.4, 28.7. HRMS calcd for $\text{C}_{37}\text{H}_{39}\text{N}_2\text{O}_7$ $[\text{M}+\text{Na}]^+$, 623.2752; found 623.2754. Specific rotation: $[\alpha]_D^{20}$ 18.0 ($c = 1.00$; MeOH).

(S)-2-amino-1-((S)-6,7-dimethoxy-1-(3,6,7-trimethoxyphenanthren-9-yl)-3,4-dihydroisoquinolin-2(1H)-yl)-3-hydroxypropan-1-one (12h)

Compound **12h** was prepared in a manner similar to that for **12a** in 40.3% yield (two steps). White solid, yield 40.3%. HPLC: 97.37%, $t_R = 10.524$ min. $^1\text{H NMR}$ (400 MHz, $\text{DMSO-}d_6$) δ 8.23 (s, 3H), 8.06 (d, $J = 2.32$ Hz, 1H), 7.83 (s, 1H), 7.64 (d, $J = 8.80$ Hz, 1H), 7.36-7.30 (m, 1H), 7.15-7.12 (m, 1H), 6.92-6.88 (m, 1H), 6.69 (d, 1H), 4.43 (s, 1H), 4.05-3.95 (m, 9H), 3.82 (s, 1H), 3.60 (s, 3H), 3.51-3.33 (m, 2H), 3.12-3.04 (m, 1H), 2.98-2.80 (m, 1H). $^{13}\text{C NMR}$ (100 MHz, $\text{DMSO-}d_6$) δ 166.8, 158.9, 150.0, 149.4, 148.6, 147.8, 132.9, 131.2, 130.8, 128.3, 127.3 (2C), 126.4, 124.8, 124.7, 116.2, 112.3, 112.0, 105.8, 104.9, 104.6, 60.8, 56.4, 56.3, 56.0, 53.6, 53.4, 53.2, 18.4, 17.1. HRMS calcd for $\text{C}_{31}\text{H}_{35}\text{N}_2\text{O}_7$ $[\text{M}+\text{H}]^+$, 547.2439; found 547.2441. Specific rotation: $[\alpha]_D^{20}$ -141.0 ($c = 1.00$; MeOH).

(S)-2-amino-1-((R)-6,7-dimethoxy-1-(3,6,7-trimethoxyphenanthren-9-yl)-3,4-dihydroisoquinolin-2(1H)-yl)-3-hydroxypropan-1-one (12i)

Compound **12i** was prepared in a manner similar to that for **12a** in 31.7% yield (two steps). White solid. HPLC: 98.83 %, $t_R = 8.912$ min. $^1\text{H NMR}$ (400 MHz, $\text{DMSO-}d_6$) δ 8.30 (s, 3H), 8.12 (s, 1H), 8.07 (d, $J = 2.08$ Hz, 1H), 7.83 (s, 1H), 7.63 (d, $J = 8.88$ Hz, 1H), 7.29 (s, 1H), 7.14 (dd, $J = 8.72, 2.28$ Hz, 1H), 6.92 (s, 1H), 6.88 (s, 1H), 6.72 (s, 1H), 4.43-4.42 (m, 1H), 4.04 (s, 1H), 3.98 (s, 1H), 3.96 (s, 1H), 3.90-3.86 (m, 1H), 3.82 (s, 1H), 3.61-3.57 (m, 4H), 3.37-3.29 (m, 1H), 3.14-3.05 (m, 1H), 2.85-2.80 (m, 1H). $^{13}\text{C NMR}$ (100 MHz, $\text{DMSO-}d_6$) δ 166.8, 158.9, 150.0, 149.4, 148.7, 147.9, 133.0, 131.2, 130.8, 128.3, 127.3 (2C), 126.4, 124.8, 124.7, 116.2, 112.3, 112.1, 105.9, 105.0, 104.6, 60.8, 56.4, 56.3, 56.0, 53.6, 53.4, 53.2, 18.4, 17.2. HRMS calcd for $\text{C}_{31}\text{H}_{34}\text{N}_2\text{O}_7\text{Na}$ $[\text{M}+\text{Na}]^+$, 569.2251; found 569.2249. Specific rotation: $[\alpha]_D^{20}$ 43.5 ($c = 1.00$; MeOH).

6-amino-1-(6,7-dimethoxy-1-(3,6,7-trimethoxyphenanthren-9-yl)-3,4-dihydroisoquinolin-2(1H)-yl)hexan-1-one (12j)

Compound **12j** was prepared in a manner similar to that for **12a** in 88.8% yield (two steps). White solid. HPLC: 98.84 %, $t_R = 10.069$ min. $^1\text{H NMR}$ (400MHz, $\text{DMSO-}d_6$) δ 8.12 (s, 1H), 8.10 (s, 1H), 8.06 (d, $J = 1.96$ Hz, 1H), 7.94 (s, 3H), 7.61 (d, $J = 8.80$ Hz, 1H), 7.33 (s, 1H), 7.12 (dd, $J = 8.76, 2.24$ Hz, 1H), 6.86 (s, 1H), 6.84 (s, 1H), 6.69 (s, 1H), 4.04 (s, 3H), 3.97 (s, 3H), 3.94 (s, 3H), 3.81 (s, 3H), 3.76-3.75 (m, 1H), 3.60 (s, 3H), 3.25-3.18 (m, 1H), 3.02-2.94 (m, 1H), 2.81-2.76 (m, 1H), 2.71 (s, 1H), 2.55-2.47 (m, 1H), 2.40-2.33 (m, 1H), 1.59-1.47 (m, 4H), 1.34-1.27 (m, 2H). $^{13}\text{C NMR}$ (100MHz, $\text{DMSO-}d_6$) δ 171.6, 158.8, 149.9, 149.3, 148.4, 147.7, 133.8, 131.1, 130.8, 127.9 (2C), 127.4, 126.6, 124.9 (2C), 116.2, 112.3, 112.0, 106.4, 105.0, 104.6, 56.4, 56.1, 56.0, 55.9 (2C), 52.6, 39.0, 38.6, 32.6, 28.4, 27.2, 26.0, 24.9. HRMS calcd for $\text{C}_{34}\text{H}_{41}\text{N}_2\text{O}_6$ $[\text{M}+\text{H}]^+$, 573.2959; found 573.2971.

tert-butyl((S)-5-amino-6-((S)-6,7-dimethoxy-1-(3,6,7-trimethoxyphenanthren-9-yl)-3,4-dihydroisoquinolin-2(1H)-yl)-6-oxohexyl)carbamate (12k)

To a solution of (*S*, *S*)-**11e** (273mg, 0.3 mmol) in acetonitrile (15 mL) was dropwise added diethylamine (3 mL). The mixture was stirred at room temperature for 2.5 h. The solvent was evaporated and the residue was purified by

column chromatography (silica gel, CH₂Cl₂/MeOH=20:1), affording product **12k** in 24.9% yield (two steps). White solid. ¹H NMR (400MHz, DMSO-*d*₆) δ 8.11 (s, 1H), 8.05 (s, 2H), 7.62 (d, *J* = 8.80 Hz, 1H), 7.34 (s, 1H), 7.12 (dd, *J* = 2.28, 8.80 Hz, 1H), 6.86 (d, *J* = 7.92 Hz, 2H), 6.69 (s, 1H), 6.65-6.62 (m, 1H), 4.04 (s, 3H), 3.98 (s, 3H), 3.94 (s, 3H), 3.81 (s, 3H), 3.78-3.74 (m, 1H), 3.68-3.64 (m, 1H), 3.60 (s, 3H), 3.25-3.22 (m, 1H), 3.12-3.03 (m, 1H), 2.81-2.76 (m, 1H), 2.70-2.68 (s, 2H), 1.32 (s, 9H), 1.24-1.19 (m, 8H). Specific rotation: [α]_D²⁰ -99.0 (c = 1.00; MeOH).

6-(5-((3*aS*,4*S*,6*aR*)-2-oxohexahydro-1*H*-thieno[3,4-*d*]imidazol-4-yl)pentanamido)hexanoic acid (15)

To a mixture of biotin (3.00 g, 12.29 mmol), methyl 6-aminohexanoate hydrochloride (2.90 g, 15.9 mmol), 1-ethyl-3-(3-dimethylaminopropyl)-carbodiimide hydrochloride (2.82 g, 14.73 mmol) and 1-hydroxybenzotriazole (1.67 g, 12.29 mmol) in dimethylformamide (30 mL) was added triethylamine (2.22 mL). The mixture was stirred for 18 h at ambient temperature. The solvent was evaporated under reduced pressure and the resulting residue was azeotroped with toluene (two times), dispersed in dichloromethane, and filtered off. The filtrate was evaporated to give compound **14**. The crude product was reacted without further purification. To a solution of compound **14** (2.36 g, 6.36mmol) in tetrahydrofuran-methanol (V/V=1:1, 24 mL) was added 2 N NaOH (6.36 mL, 12.7 mmol) solution at ambient temperature. The mixture was stirred for 20 h, chilled in an ice bath and neutralized by adding concentrated hydrochloric acid (1.06 mL). A white precipitate was formed and the mixture was diluted with tetrahydrofuran. The precipitate was collected by filtration, washed with tetrahydrofuran and dried to give compound **15** (1.98 g, 35% for two steps). ¹H-NMR (400MHz, DMSO-*d*₆) δ 11.98(s, 1H), 7.73-7.76 (m, 1H), 6.42(s, 1H), 6.36 (s, 1H), 4.29-4.33(m, 1H), 4.12-4.15 (m, 1H), 3.09-3.11(m, 1H), 2.99-3.03(m, 2H), 2.83 (dd, *J*=12.40, 5.04 Hz, 1H), 2.59 (d, *J*=12.40 Hz, 1H), 2.19 (t, *J*=7.36 Hz, 2H), 2.05 (t, *J*=7.32 Hz, 2H), 1.23-1.61(m, 12H). ¹³C-NMR (100MHz, DMSO-*d*₆) δ 174.9, 172.3, 163.2, 61.5, 24.7, 59.7, 55.9, 40.3, 38.7, 35.7, 34.1, 29.4, 28.7, 28.5, 26.5, 25.8. *m/z* (ES-) (M-H)⁻ =356.34.

tert-butyl((S)-6-((S)-6,7-dimethoxy-1-(3,6,7-trimethoxyphenanthren-9-yl)-3,4-dihydroisoquinolin-2(1*H*)-yl)-6-oxo-5-(6-(5-((3*aS*,4*S*,6*aR*)-2-oxohexahydro-1*H*-thieno[3,4-*d*]imidazol-4-yl)pentanamido)hexanamido)hexyl)carbamate (16)

A mixture of compound **15** (357.2 mg, 1 mmol), compound **12k** (687.4 mg, 1 mmol), 1-hydroxybenzotriazole (202.5 mg, 1.5 mmol), *N,N*-diisopropylethylamine (0.33 mL, 2 mmol), 1-Ethyl-3-(3-dimethylaminopropyl)-carbodiimide hydrochloride (286.5 mg, 1.5 mmol), in dimethylformamide (32 mL) was stirred for 24 h at ambient temperature. After addition of water, the precipitate was collected by filtration, washed with water and dried to give a gray solid. The crude product was purified by column chromatography (silica gel, CH₂Cl₂/MeOH=25:1 as eluent) to yield compound **16** as a white solid (0.97 g, 95%). ¹H NMR (400MHz, DMSO-*d*₆) δ 8.14-8.16(d, *J* = 8.16 Hz, 1H), 8.12(s, 1H), 8.07(s, 1H), 8.01(s, 1H), 7.72(s, 1H), 7.63(d, *J* = 8.48 Hz, 1H), 7.31(s, 1H), 7.12 (d, *J* = 8.08 Hz, 1H), 6.88(s, 1H), 6.86(s, 1H), 6.66(s, 2H), 6.43(s, 1H), 6.36(s, 1H), 4.78(s, 1H), 4.30(s, 1H), 4.12(s, 1H), 4.04(s, 3H), 3.98(s, 3H), 3.96(s, 3H), 3.82(m, 4H), 3.60(s, 3H), 3.15-3.30(m, 2H), 3.00-3.07(m, 3H), 2.80(s, 2H), 2.70(s, 2H), 2.58 (d, *J* = 12.44 Hz, 1H), 2.05-2.13(m, 4H), 1.08-1.60(m, 27H). ¹³C NMR (100MHz, DMSO-*d*₆) δ 22.9, 25.4, 25.8 (2C), 26.6, 28.5, 28.7(2C), 29.4 (2C), 29.5 (2C), 32.4, 35.4, 35.7, 38.8, 49.0, 52.9, 55.4, 55.9(2C), 56.0(3C), 56.1, 56.4(2C), 59.7, 61.5, 77.7, 104.6, 105.1, 106.1, 112.1, 112.3, 116.2, 124.9 (2C), 126.5, 127.6, 127.6, 128.1, 130.8, 131.1, 133.7, 147.7, 148.5, 149.3, 149.9, 155.9, 158.9, 163.2, 171.7, 172.2, 172.4. HRMS calcd for C₅₅H₇₄N₆O₁₁SNa, [M+Na]⁺, 1049.5028; found 1049.5013.

***N*-((S)-6-amino-1-((S)-6,7-dimethoxy-1-(3,6,7-trimethoxyphenanthren-9-yl)-3,4-dihydroisoquinolin-2(1*H*)-yl)-1-oxohexan-2-yl)-6-(5-((3*aS*,4*S*,6*aR*)-2-oxohexahydro-1*H*-thieno[3,4-*d*]imidazol-4-yl)pentanamido)hexanamide hydrochloride (17)**

A mixture of compound **16** (380 mg, 0.37 mmol) in 1M HCl solution in ethyl acetate (10 mL) was stirred for 4 h at

ambient temperature. The precipitate was collected by filtration, washed with diethyl ether to yield compound **17** (biotinconjugated **12a**) as a white solid (337 mg, 94.6%). ¹H NMR (400MHz, DMSO-*d*₆) δ 8.23(d, *J* = 8.12 Hz, 1H), 8.13(s, 1H), 8.07(d, *J* = 1.76 Hz, 1H), 8.02(s, 1H), 7.88(s, 3H), 7.78 (t, *J* = 5.36 Hz, 1H), 7.63(d, *J* = 8.88 Hz, 1H), 7.32(s, 1H), 7.14 (dd, *J* = 8.72, 2.12 Hz, 1H), 6.88 (d, *J* = 7.08 Hz, 2H), 6.67(s, 1H), 6.66(s, 1H), 6.43(s, 1H), 4.77-4.82(m, 1H), 4.28-4.31(m, 1H), 4.10-4.13(m, 1H), 4.05(s, 3H), 3.98(s, 3H), 3.97(s, 3H), 3.86-3.88(m, 4H), 3.60(s, 3H), 3.27-3.33(m, 1H), 3.04-3.17(m, 2H), 2.97-3.02(m, 2H), 2.54-2.59(m, 3H), 2.03-2.20(m, 4H), 1.09-1.64(m, 18H). ¹³C NMR (400MHz, DMSO-*d*₆) δ 172.5, 172.3, 163.2, 158.9, 149.9, 149.3, 148.5, 147.7, 133.7, 131.1, 130.8, 128.1, 127.6, 127.5, 126.5, 124.9(2C), 116.2, 112.2, 112.1, 106.2, 105.1, 104.6, 61.5 (2C), 59.7, 56.4, 56.2 (2C), 56.1 (2C), 56.0, 55.9 (2C), 52.9, 48.8, 38.7 (2C), 35.7, 35.4, 32.1, 29.4, 28.7 (2C), 28.5, 27.0, 26.6, 25.8, 25.4, 22.5. HRMS calcd for C₅₀H₆₆N₆O₉SNa, [M+Na]⁺, 949.4504; found 949.4496.

Electronic circular dichroism (ECD) spectra

ECD spectrum were recorded on a Bio-logic MOS 450 spectropolarimeter as MeOH solutions (0.5 mg/mL) and were solvent subtracted. The 3D structures of compounds were generated via CORINA, a fast and powerful 3D structure generator. A series of geometry optimizations were performed by the semi-empirical method PM6, followed by a Hatree-Fock calculation at the HF/6-31G (d) level then by the density functional theory method at the B3LYP/6-31G (d) level in vacuum and in methanol with the CPCM model in Gaussian 09 program package.³⁴ They were further checked by frequency calculations and resulted in no imaginary frequencies. The ECDs of compound were then calculated by the TDDFT method at the B3LYP/6-31+G(d, p) level with the CPCM model in methanol solution. The calculated ECD curves were extracted and Boltzmann averaged using SpecDis 1.62³⁵ with $\sigma = 0.30$ eV.

Biology

Kinase assay

PAK4 was preincubated with the indicated concentrations of all the compounds for 30 minutes at 30°C, then the kinase assay were performed using the exogenous and a mixture of 1 mM ATP and [γ -³²P] ATP(5000 Ci/mmol). Kinase reactions were started by addition of Histone H3. Reactions were stopped by addition of 6×SDS buffer and loading on a 12% SDS-PAGE. Proteins were transferred onto PVDF membranes and ³²P-labelled proteins were visualized by autoradiography with Molecular Imager RX (BIO-RAD). To assure equal loading amount, PAK4 were detected by immunoblotting analysis and Histone H3 (Roche) was detected by ponceau stain.

Cell Proliferation assay

The human breast cell line MCF-7, the human pulmonary carcinoma cell line A-549 and the human fibrosarcoma cell line HT-1080 were cultured in RPMI-1640 medium containing 10% FBS, 100 U/mL streptomycin and 100 U/mL penicillin at 37°C in a humidified atmosphere containing 5% CO₂.

The *in vitro* anti-proliferative activities of the target compounds were determined with an MTT assay. MCF-7, A549, and HT1080 cells (1×10⁴/well) were plated in 0.1 mL of the medium containing 10% FBS in 96-well Corning plates; 24h later, the medium was removed and replaced with 0.1 mL medium containing the indicated concentrations of the target compounds for 24h. At the end of the incubation, the capability of cellular proliferation was measured by the modified tetrazolium salt 3-(4, 5-dimethylthiazol-2-yl)-2, 5-biphenyl-tetrazolium bromide (MTT, Sigma) assay. For this, 0.01 mL of MTT solution (5 mg/mL in PBS) was added to each well. After a 4h incubation at 37°C, medium was replaced by 0.15 mL DMSO. After 15 min incubation at 37°C, the optical densities at 595 nm were measured using a Microplate Reader (BIO-RAD). The data were calculated and plotted as the percent viability compared to the control. The 50% inhibitory concentration (IC₅₀) was defined as the concentration that reduced the absorbance of the untreated wells by 50% of the vehicle in the MTT assay.

Cell-cycle analysis by flow cytometry

A549 cells (8×10^4 cells) were incubated with the indicated concentrations of **12a** for 24 h. After incubation, cells were collected, washed with PBS and then suspended in a staining buffer (10 $\mu\text{g}/\text{mL}$ propidium iodide, 0.5% Tween-20, 0.1% RNase in PBS). The cells were analyzed using a FACSVantage flow cytometer with the Cell Quest acquisition and analysis software program (Becton Dickinson and Co., San Jose, CA).

Analysis of cell apoptosis

The ability of **12a** to induce cell apoptosis of A549 cells was quantified by annexin-V and PI staining and flow cytometry, as described previously. Briefly, after treatment with **12a** for 24 h, cells were collected and washed with PBS twice, and subjected to annexin-V and propidium iodide staining using annexin-V FITC apoptosis kit following the step-by-step protocol provided by the manufacturer. After staining, flow cytometry was performed for the quantification of apoptotic cells.

Cell invasion assay

Matrigel invasion assays were performed using modified Boyden chambers with polycarbonate nucleopore membrane. Precoated filters (6.5 mm in diameter, 8 μm pore size, and Matrigel 100 $\mu\text{g}/\text{cm}^2$) were rehydrated with 100 μL medium. Then, 1×10^5 cells in 100 μL serum-free DMEM supplemented with 0.1% bovine serum albumin were placed in the upper part of each chamber, whereas the lower compartments were filled with 600 μL DMEM containing 10% serum. After incubating for 18 h at 37°C, non-invaded cells were removed from the upper surface of the filter with a cotton swab, and the invaded cells on the lower surface of the filter were fixed, stained, photographed and counted under high-power magnification.

Lentiviral production and infection

Recombinant lentiviruses including PAK4-Lentivirus, PAK4-RNAi-Lentivirus and pGC FU-GFP-LV, NC-GFP-LV vectors were purchased from Shanghai GeneChem Company. To stably overexpress PAK4, cells were infected with lentivirus carrying PAK4, and then selected with puromycin (1.5 $\mu\text{g}/\text{mL}$). The pGC FU-GFP-LV vector was used as control.

Western blot analysis

To determine the expression of protein, whole cell extracts were prepared from 1×10^6 cells in RIPA lysis buffer (50 mM Tris/HCl pH 7.4, 150 mM NaCl, 1% Nonidet P-40, 0.25% Na-deoxycholate, 1 mM EDTA and protease inhibitor cocktail). Equal amounts of denatured protein were separated by SDS-PAGE and transferred to a PVDF membrane (Millipore). The membrane was blocked with 5% nonfat dry milk in TBS-T (20 mM Tris, pH 7.4, 137 mM NaCl, 0.05% Tween-20) for 3 h at room temperature, and the proteins were probed with specific antibodies: CDK2, CDK6, cyclinD3, Bcl-2, BAX, caspase 3, caspase 8, LIMK1, phospho-LIMK1, cofilin, phospho-cofilin, PAK4, phospho-PAK4/Ser474. All PVDF membranes were detected by chemiluminescence (ECL, Pierce Technology). To assure equal loading, membranes were stripped and reprobed with antibody against GAPDH and MMP2 (Shang Hai Kangchen).

Immunoprecipitation assay

To determine binding of compound **12a** with PAK4, A549 cells transfected with pCDNA3.1-3 \times Flag-PAK4 (WT), pCDNA3.1-3 \times Flag-PAK4 (1-325aa) or pCDNA3.1-3 \times Flag-PAK4 (326-592aa) were incubated with **17** (biotin-labeled **12a**) (500 nmol) for 12 h. Cells were washed with ice-cold PBS twice before being lysed in IP lysis buffer (25 mM Tris pH 7.4, 150 mM NaCl, 1% Nonidet P-40, 1 mM EDTA) supplemented with proteinase and phosphatase inhibitors (2 mM dithiothreitol, 1 mM phenylmethylsulfonyl fluoride, 10 $\mu\text{g}/\text{mL}$ leupeptin, 10 $\mu\text{g}/\text{mL}$ aprotinin, 20 mM glycerophosphate, 1 mM Na_3VO_4). Total cell lysate was immunoprecipitated with sepharose beads (streptavidin conjugate) at 4 °C overnight. The precipitated proteins were denatured in 2 \times SDS loading buffer, separated by SDS-PAGE, transferred to PVDF membrane (Millipore). The membrane was blocked with 5% nonfat dry milk in TBS-T (20 mM Tris, pH 7.4, 137 mM NaCl, 0.05% Tween-20) for 3 h at room temperature, and the proteins were probed with anti-Flag antibody for 3hr at room temperature. All PVDF membranes were detected by

chemiluminescence (ECL, Pierce Technology). Total cell lysates were loaded as input to indicate the immunoprecipitated proteins.

In Vivo Antitumor Activity Assay

Male and female nude mice (4-6 weeks) were housed in a specific pathogen-free room with a 12 h light/dark schedule at 25 °C and were fed an autoclaved chow diet and water. The present study was carried out in accordance with guidelines for animal experiments in Shenyang Pharmaceutical University, and the experimental protocols were approved by the Animal Care Committee of the institution. The cells at a density of $(5-10) \times 10^6$ in 200 μL were first implanted sc into the right flank of each nude mouse and then allowed to grow to 600-700 mm^3 , defined as a well-developed tumor. After that, the well-developed tumors were cut into 1 mm^3 fragments and transplanted sc into the right flank of nude mice. When the tumor volume reached 80-100 mm^3 , the mice were randomly assigned into control and treatment groups ($n = 5$ in treated group, $n = 10$ in vehicle group). Control groups were given vehicle alone, and treatment groups received compound **12a** with indicated doses via oral administration or doxorubicin with EtOH and water via oral administration once daily for 2 weeks. The weights of the tumors were measured twice per week. Data was shown on indicated days. Percent (%) inhibition values were measured on the final day of study for drug-treated compared with vehicle-treated mice and are calculated.

Conclusions

In this work, a novel series of 1-phenanthryl-tetrahydroisoquinoline derivatives showed significant PAK4 inhibition and anti-proliferation effect. A set of systematic and in-deep profiling assays both *in vitro* and *in vivo* was employed to investigate the mechanisms and efficacy of the compound. Compound **12a** was found to regulate cellular functions *in vitro* and *in vivo*, including regulation of cell invasion, cell cycle and apoptotic processes in cancer cells. To further evaluate the binding mode of **12a** with PAK4, biotinylated **12a** derivative has been synthesized and was used for immunoprecipitation assay. Our observations suggest that **12a** interactions with both the N- and C-termini of PAK4.

Acknowledgments

We gratefully acknowledge the financial support from the National Natural Science Foundation of China (Grant 1230077, 81102379, 81001092, and J1210029), the National High Technology Research and Development Program of China (Grant 2007AA02Z305) and Program for Innovative Research Team of the Ministry of Education, and Program for Liaoning Innovative Research Team in University.

Notes and references

1. E. Manser, T. Leung, H. Salihuddin, Z. S. Zhao and L. Lim, *Nature*, 1994, **367**, 40-46.
2. E. Leberer, C. Wu, T. Leeuw, A. Fourest-Lieuvin, J. E. Segall and D. Y. Thomas, *EMBO J.*, 1997, **16**, 83-97.
3. J. W. Harper, G. R. Adami, N. Wei, K. Keyomarsi and S. J. Elledge, *Cell*, 1993, **75**, 805-816.
4. Z. S. Zhao and E. Manser, *Biochem. J.*, 2005, **386**, 201-214.
5. L. E. Arias-Romero and J. Chernoff, *Biol. Cell*, 2008, **100**, 97-108.
6. B. Dummler, K. Ohshiro, R. Kumar and J. Field, *Cancer Metastasis Rev.*, 2009, **28**, 51-63.
7. J. Qu, X. Li, B. G. Novitch, Y. Zheng, M. Kohn, J. M. Xie, S. Kozinn, R. Bronson, A. A. Beg and A. Minden, *Mol. Cell. Biol.*, 2003, **23**, 7122-7133.
8. Y. Baskaran, Y. W. Ng, W. Selamat, F. T. Ling and E. Manser, *EMBO Rep.*, 2012, **13**, 653-659.
9. A. Whale, F. N. Hashim, S. Fram, G. E. Jones and C. M. Wells, *Front. Biosci. (Landmark Ed)*, 2011, **16**, 849-864.
10. D. Z. Ye and J. Field, *Cell. Logist.*, 2012, **2**, 105-116.

11. J. Rudolph, J. J. Crawford, K. P. Hoeflich and W. Wang, *J. Med. Chem.*, 2015, **58**, 111-129.
12. A. E. Dart and C. M. Wells, *Eur. J. Cell. Biol.*, 2013, **92**, 129-138.
13. A. Abo, J. Qu, M. S. Cammarano, C. Dan, A. Fritsch, V. Baud, B. Belisle and A. Minden, *EMBO J.*, 1998, **17**, 6527-6540.
14. D. W. Parsons, T. L. Wang, Y. Samuels, A. Bardelli, J. M. Cummins, L. DeLong, N. Silliman, J. Ptak, S. Szabo, J. K. Willson, S. Markowitz, K. W. Kinzler, B. Vogelstein, C. Lengauer and V. E. Velculescu, *Nature*, 2005, **436**, 792.
15. E. H. Mahlamaki, P. Kauraniemi, O. Monni, M. Wolf, S. Hautaniemi and A. Kallioniemi, *Neoplasia*, 2004, **6**, 432-439.
16. A. Begum, I. Imoto, K. Kozaki, H. Tsuda, E. Suzuki, T. Amagasa and J. Inazawa, *Cancer Sci.*, 2009, **100**, 1908-1916.
17. M. G. Callow, F. Clairvoyant, S. Zhu, B. Schryver, D. B. Whyte, J. R. Bischoff, B. Jallal and T. Smeal, *J. Biol. Chem.*, 2002, **277**, 550-558.
18. Y. Liu, N. Chen, X. Cui, X. Zheng, L. Deng, S. Price, V. Karantza and A. Minden, *Oncogene*, 2010, **29**, 5883-5894.
19. D. Li, Y. Zhang, Z. Li, X. Wang, X. Qu and Y. Liu, *Tumour Biol.*, 2015, **36**, 9431-9436.
20. S. Cai, Z. Ye, X. Wang, Y. Pan, Y. Weng, S. Lao, H. Wei and L. Li, *J. Exp. Clin. Cancer Res.*, 2015, **34**, 48.
21. C. Dan, A. Kelly, O. Bernard and A. Minden, *J. Biol. Chem.*, 2001, **276**, 32115-32121.
22. C. Kuijl, N. D. Savage, M. Marsman, A. W. Tuin, L. Janssen, D. A. Egan, M. Ketema, R. van den Nieuwendijk, S. J. van den Eeden, A. Geluk, A. Poot, G. van der Marel, R. L. Beijersbergen, H. Overkleeft, T. H. Ottenhoff and J. Neefjes, *Nature*, 2007, **450**, 725-730.
23. B. J. Ryu, H. Lee, S. H. Kim, J. N. Heo, S. W. Choi, J. T. Yeon, J. Lee, J. Y. Cho and S. Y. Lee, *Mol. Cell. Biochem.*, 2014, **389**, 69-77.
24. X. Li and A. Minden, *J. Biol. Chem.*, 2005, **280**, 41192-41200.
25. Y. Li, Y. Shao, Y. Tong, T. Shen, J. Zhang, H. Gu and F. Li, *Biochim. Biophys. Acta.*, 2012, **1823**, 465-475.
26. T. W. Kim, Y. K. Kang, Z. Y. Park, Y. H. Kim, S. W. Hong, S. J. Oh, H. A. Sohn, S. J. Yang, Y. J. Jang, D. C. Lee, S. Y. Kim, H. S. Yoo, E. Kim, Y. I. Yeom and K. C. Park, *Carcinogenesis*, 2014, **35**, 624-634.
27. N. Gnesutta, J. Qu and A. Minden, *J. Biol. Chem.*, 2001, **276**, 14414-14419.
28. R. Kumar, A. E. Gururaj and C. J. Barnes, *Nat. Rev. Cancer*, 2006, **6**, 459-471.
29. B. Guo, X. Li, S. Song, M. Chen, M. Cheng, D. Zhao and F. Li, *Oncol. Rep.*, 2016, **35**, 2246-2256.
30. S. Song, X. Li, J. Guo, C. Hao, Y. Feng, B. Guo, T. Liu, Q. Zhang, Z. Zhang, R. Li, J. Wang, B. Lin, F. Li, D. Zhao and M. Cheng, *Org. Biomol. Chem.*, 2015, **13**, 3803-3818.
31. P. F. Yu, H. N. Lv, C. Li, J. H. Ren, S. G. Ma, S. Xu, X. G. Chen and S. S. Yu, *Synthesis-Stuttgart*, 2012, **44**, 3757-3764.
32. L.Y. Kong and P. Wang, *Chin. J. Nat. Med.*, 2013, **11**, 193-198.
33. M. Wilchek and E. A. Bayer, *Methods. Enzymol.*, 1990, **184**, 123-138.
34. Gaussian 09, Revision D.01, M. J. Frisch, G. W. Trucks, H. B. Schlegel, G. E. Scuseria, M. A. Robb, J. R. Cheeseman, G. Scalmani, V. Barone, B. Mennucci, G. A. Petersson, H. Nakatsuji, M. Caricato, X. Li, H. P. Hratchian, A. F. Izmaylov, J. Bloino, G. Zheng, J. L. Sonnenberg, M. Hada, M. Ehara, K. Toyota, R. Fukuda, J. Hasegawa, M. Ishida, T. Nakajima, Y. Honda, O. Kitao, H. Nakai, T. Vreven, J.A. Montgomery, Jr., J.E. Peralta, F. Ogliaro, M. Bearpark, J. J. Heyd, E. Brothers, K. N. Kudin, V. N. Staroverov, T. Keith, R. Kobayashi, J. Normand, K. Raghavachari, A. Rendell, J. C. Burant, S. S. Iyengar, J. Tomasi, M. Cossi, N. Rega, J. M. Millam, M. Klene, J. E. Knox, J. B. Cross, V. Bakken, C. Adamo, J. Jaramillo, R. Gomperts, R. E. Stratmann, O. Yazyev, A. J. Austin, R. Cammi, C. Pomelli, J. W. Ochterski, R. L. Martin, K. Morokuma, V. G. Zakrzewski, G. A.

- Voth, P. Salvador, J. J. Dannenberg, S. Dapprich, A. D. Daniels, O. Farkas, J. B. Foresman, J. V. Ortiz, J. Cioslowski, D. J. Fox, Gaussian, Inc., Wallingford CT, 2013.
35. Spec Dis, version 1.62, T. Bruhn, Y. Hemberger, A. Schaumlöffel, G. Bringmann, University of Würzburg, Germany, 2014.